Dark Matter in Galaxy Clusters

Shape, Projection, and Environment

Austen M. Groener

Drexel University

September 10, 2015

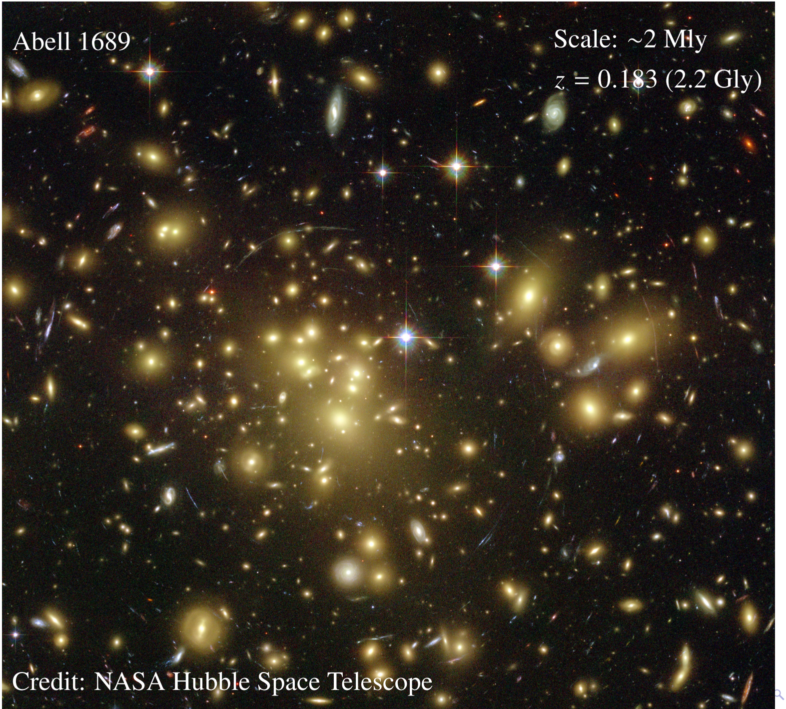
Abell 1689
Scale: ~2 Mly
z = 0.183 (2.2 Gly)
Credit: NASA Hubble Space Telescope

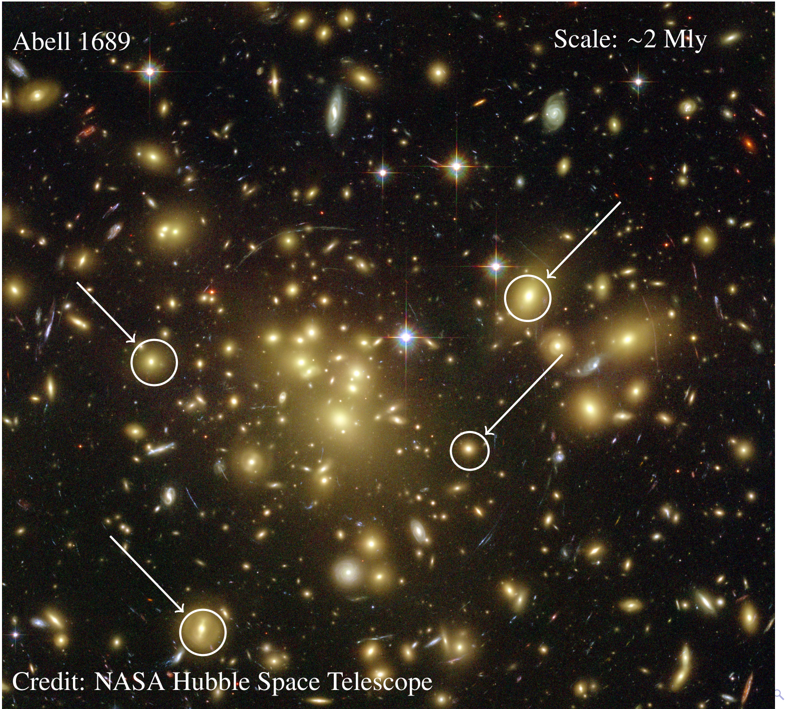
Abell 1689
Scale: ~2 Mly
Credit: NASA Hubble Space Telescope


Abell 1689
Scale: ~2 Mly
Credit: X-ray: NASA/CXC/MIT/E.-H Peng et al
Optical: NASA/STScI

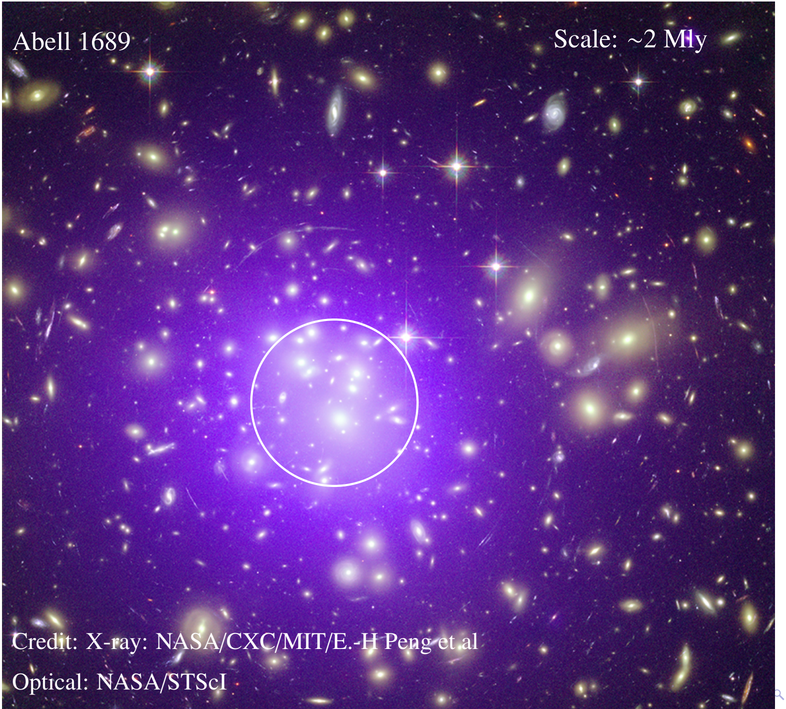
Abell 1689
Scale: ~2 Mly
Credit: X-ray: NASA/CXC/MIT/E.-H Peng et al
Optical: NASA/STScI

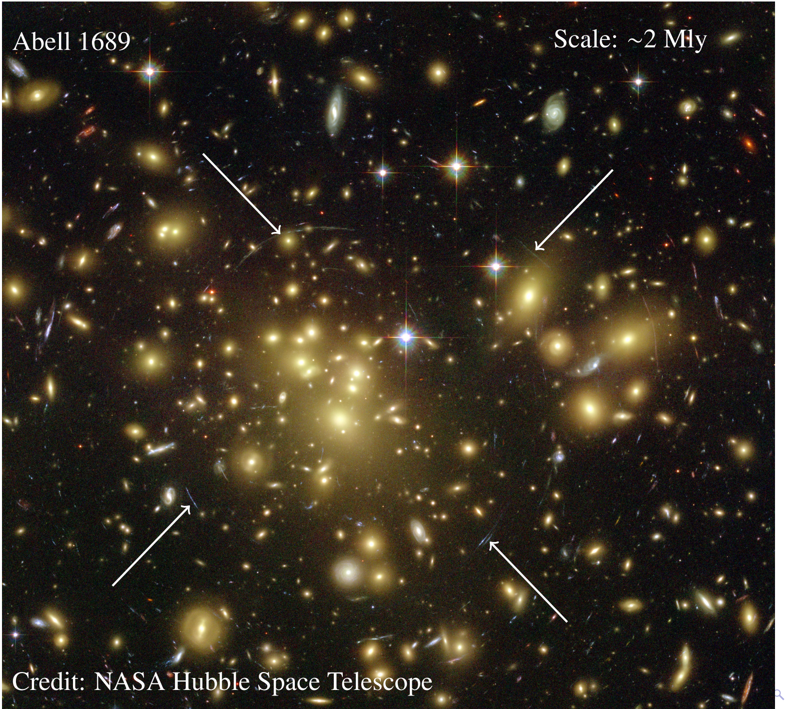
Abell 1689
Scale: ~2 Mly
Credit: NASA Hubble Space Telescope

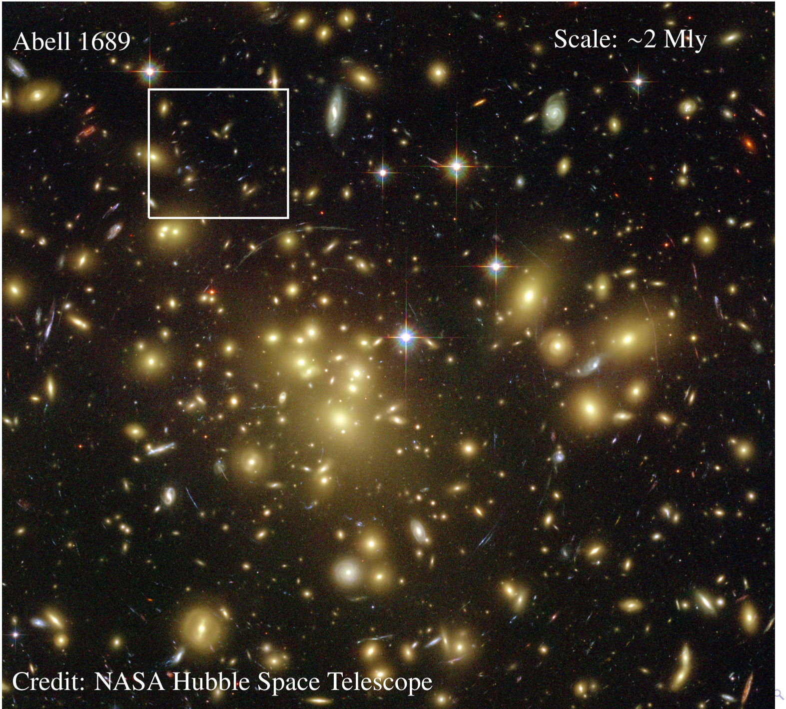
Abell 1689
Scale: ~2 Mly
Credit: NASA Hubble Space Telescope

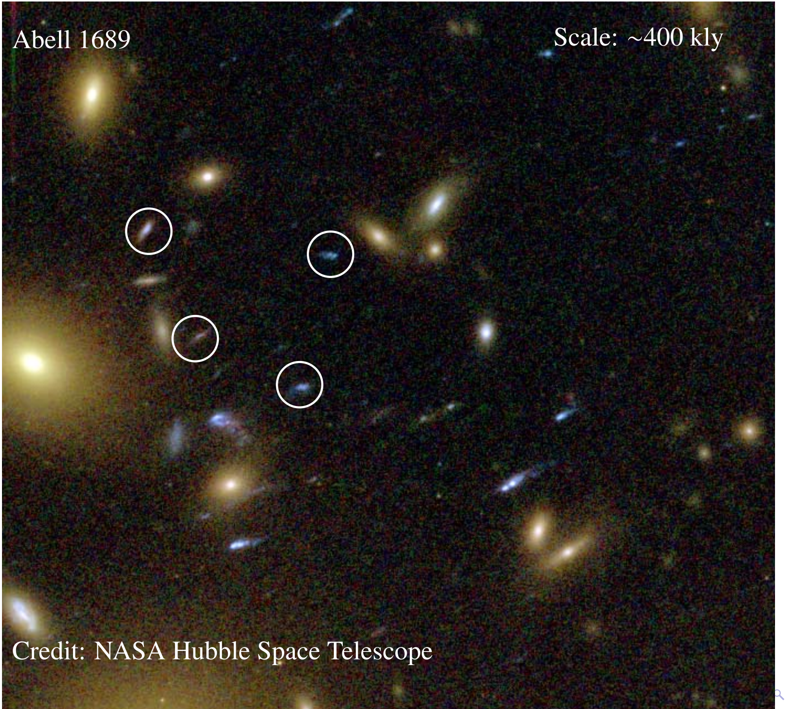
Abell 1689
Scale: ~400 kly
Credit: NASA Hubble Space Telescope

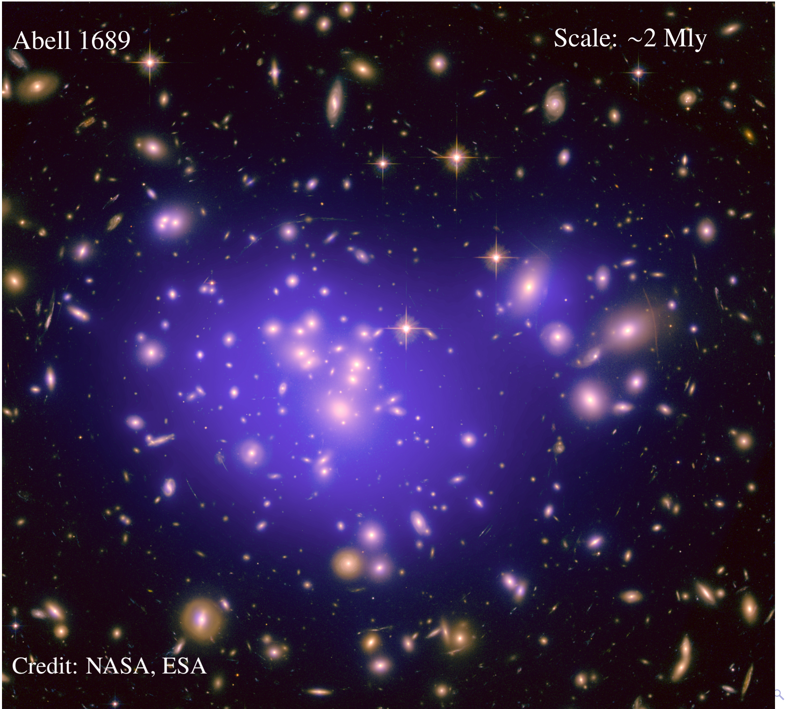
Abell 1689
Scale: ~2 Mly
Credit: NASA, ESA

Hierarchical Structure Formation

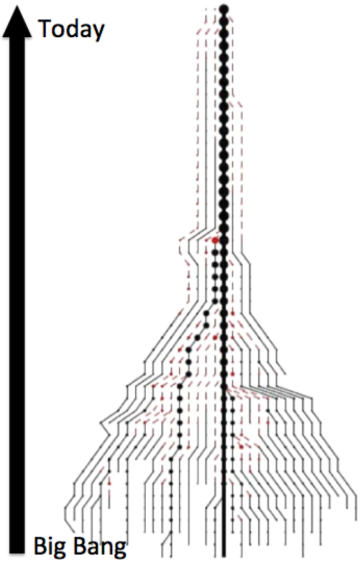

Stewart et al. (2008)

Hierarchical Structure Formation

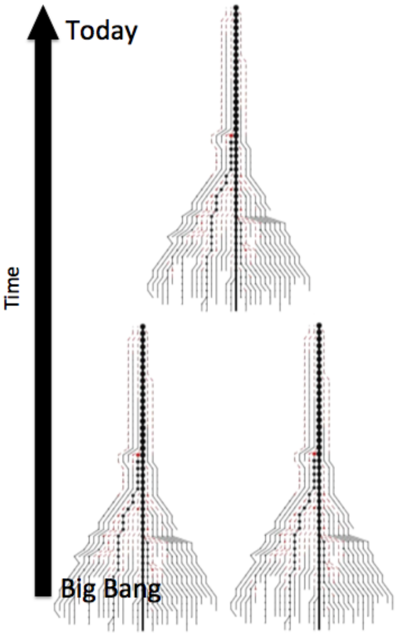

The Navarro-Frenk-White Profile

NFW (1996)

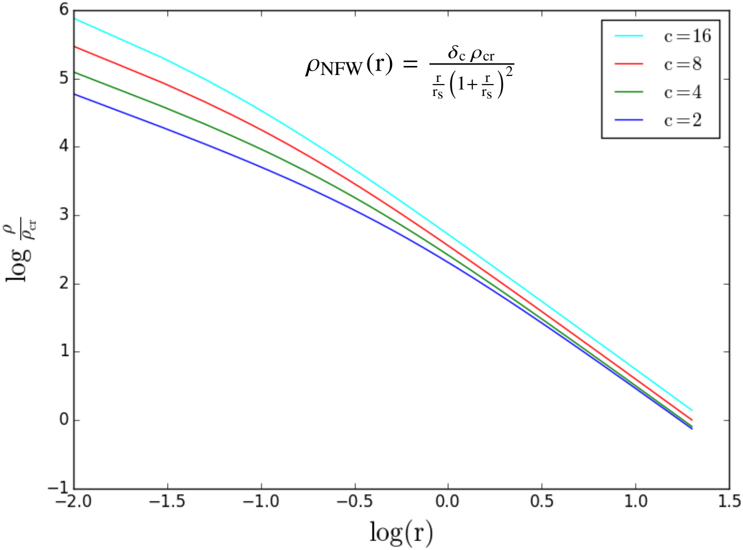

The Navarro-Frenk-White Profile

NFW (1996)

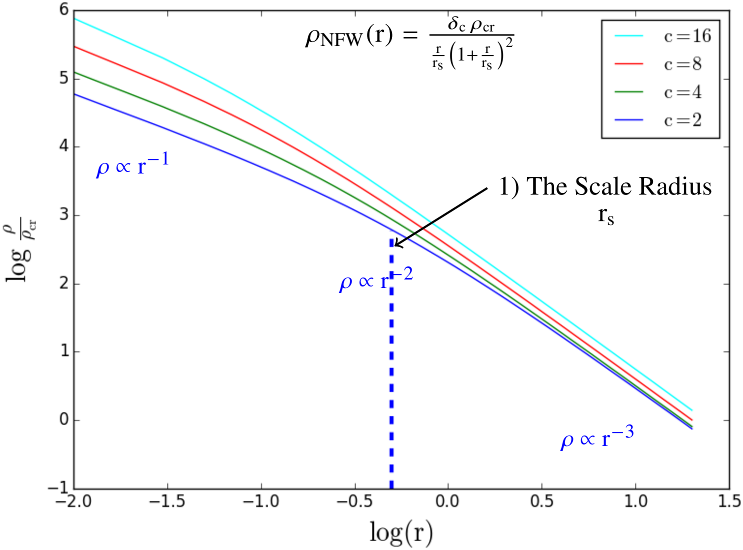

The Navarro-Frenk-White Profile

NFW (1996)

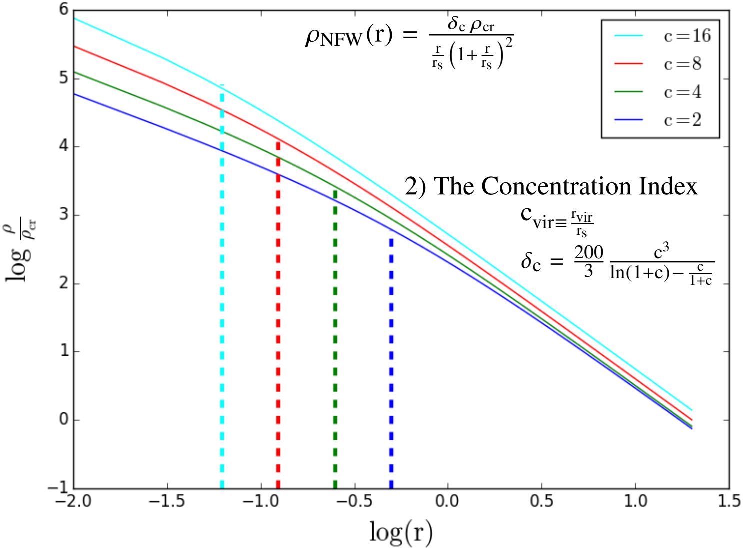

The Cuspy Halo Problem

(The Over-Concentration Problem)

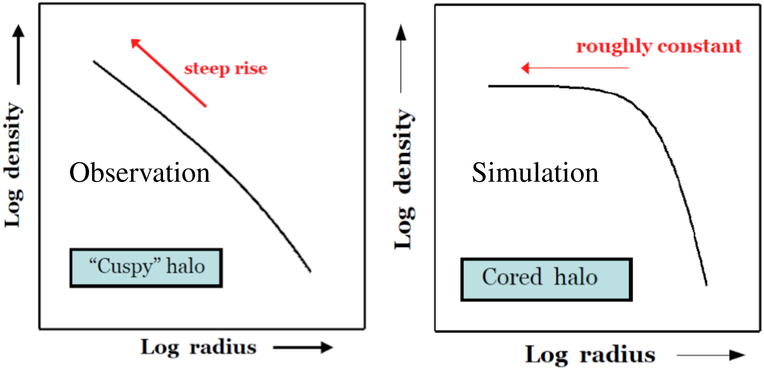

- Observed clusters: $c_{vir} = 8 - 12$
- Simulated clusters: $c_{vir} = 4 - 6$

The Concentration-Mass (c-M) Scaling Relation

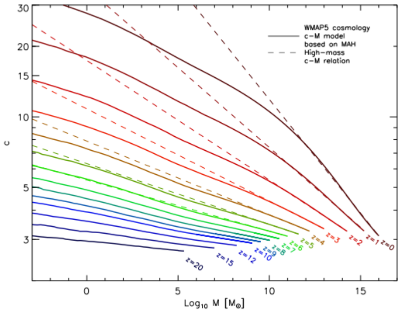

Simulation (Correa et al. 2015)

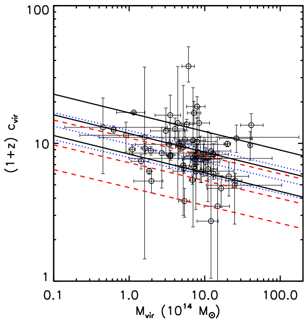

Observational (Comerford & Natarajan 2007)

Clusters Are *Not* Spherical

Triaxial Ellipsoid

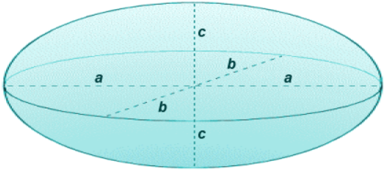

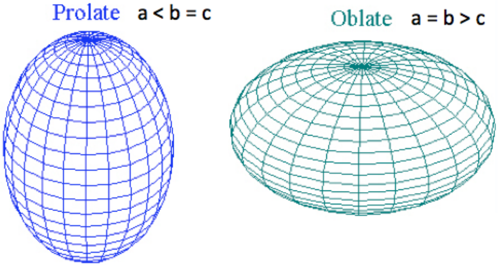

Triaxial Projection Biases 2D Observables

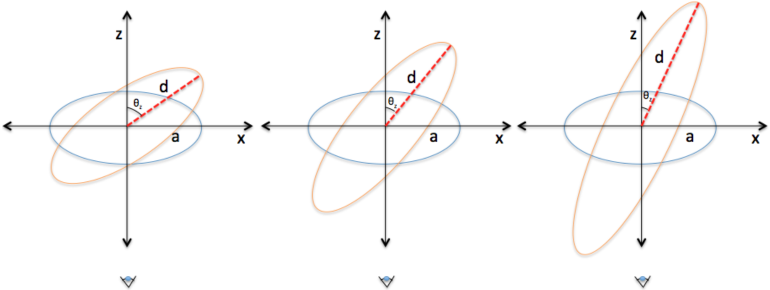

Simulated Halo Isodensities Are Not Constant On All Scales

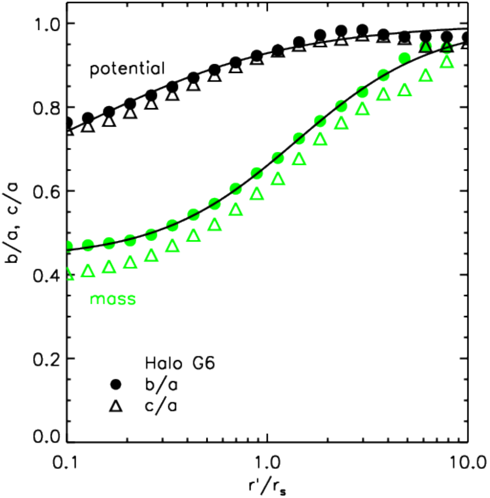

Hayashi et al. (2007)

Implications For Cluster Mass Reconstruction

- Does the changing of isodensity shape affect the concentration parameter *differently* as a function of cluster scale?
- Is the 2D concentration even a well-defined quantity?

Groener & Goldberg (2014)

The MDR1 Simulation (Prada et al. 2012)

- Dark matter only, 2048^3 particles
- Adaptive-Refinement-Tree (ART) (Kravtsov et al. 1997)
- Cosmology: WMAP5
- Mass resolution: $8.721 \times 10^9\ M_\odot/h$
- Force resolution: 7.0 kpc/h
- Box: 1000 Mpc/h (on a side)
- Mass range: $(1.7 \times 10^{11} - 1.6 \times 10^{15})\ M_\odot/h$

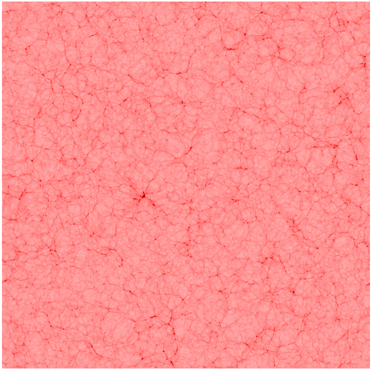

MDR1 Simulated Cluster Halos

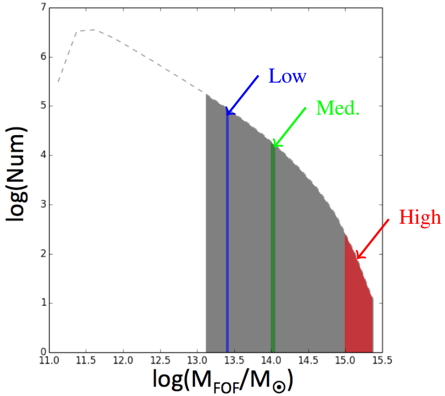

The Sample (z=0)

- Low Mass: $(2.5 - 2.6) \times 10^{13} M_\odot/h$ [6007]
- Med. Mass: $(1.0 - 1.1) \times 10^{14} M_\odot/h$ [2905]
- High Mass: $> 1.0 \times 10^{15} M_\odot/h$ [121]

Sample Selection Criteria

Clustering and Virialization Criteria

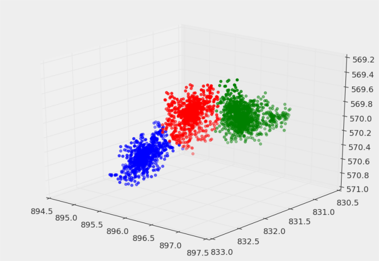

Merging, unrelaxed cluster

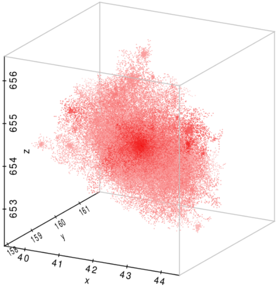

The Final Product

- MDR1 Friends of Friends (FOF) Catalog
- Apply MeanShift/K-Means Algorithms

- Find Dynamically Relaxed Halos Shaw et al. (2006)

Full Distribution of Shapes

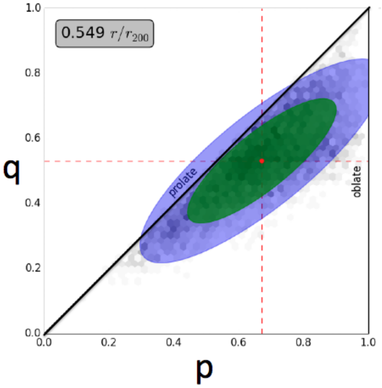

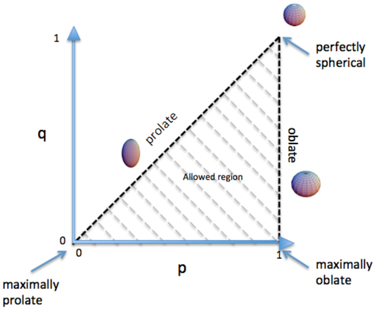

Changing Shape of Isodensities

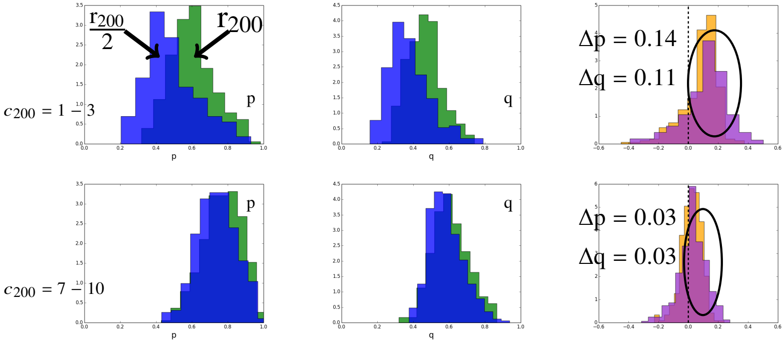

Along the Top: Distribution of axial ratios p, q, on characteristic scales $r_{200}/2$ (blue), and r_{200} (green) for $c_{200} = 1 - 3$. Difference in axial ratios p (purple) and q (orange) on these scales. *Along the Bottom*: Similar plots for $c_{200} = 7 - 10$.

Concentrations In Projection

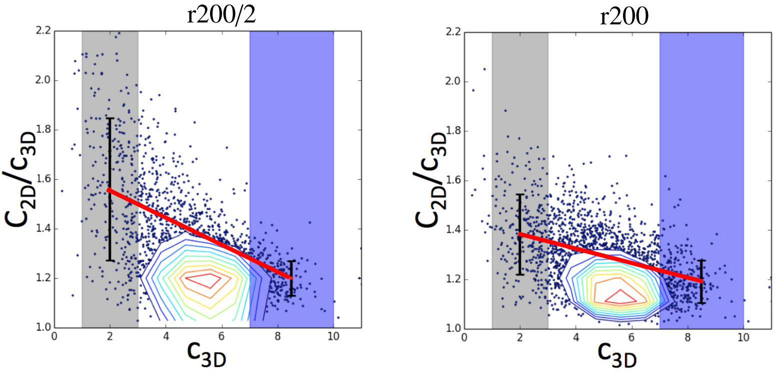

- Trend 1: Projected concentration is a function of intrinsic concentration, and is fractionally larger for low concentrations.

Concentrations In Projection

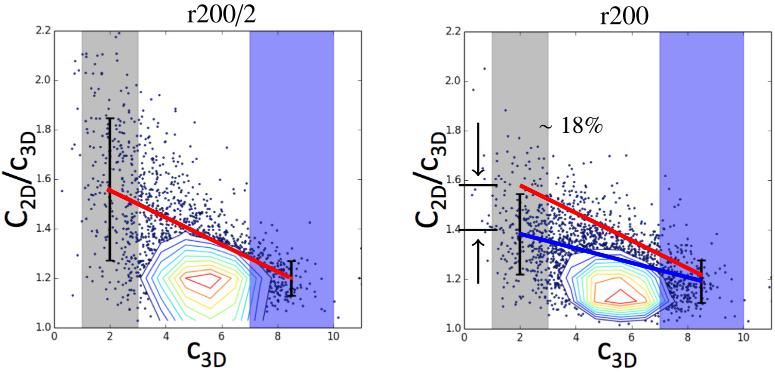

- Trend 2: Projected concentration is a function of radius, and changes the most for intrinsically low concentrations.

Conclusions

- Relaxed MDR1 cluster halos are prolate spheroidal in shape, and move toward sphericity at larger radii.
- Due to analytical projection, line-of-sight oriented halos are over-concentrated.
- This over-concentration is stronger on SL scales than on WL scales ($\sim 20\%$).
- Lower mass halos ($\sim 3 \times 10^{13}\,\mathrm{h}^{-1}\mathrm{M}_{\odot}$) are *more* affected by this difference than high mass halos are.

THE ASTROPHYSICAL JOURNAL

SHAPE PROFILES AND ORIENTATION BIAS FOR WEAK AND STRONG LENSING CLUSTER HALOS

A. M. Groener and D. M. Goldberg

Published 2014 October 23 • • The Astrophysical Journal, Volume 795, Number 2

The c-M Relation: What To Expect

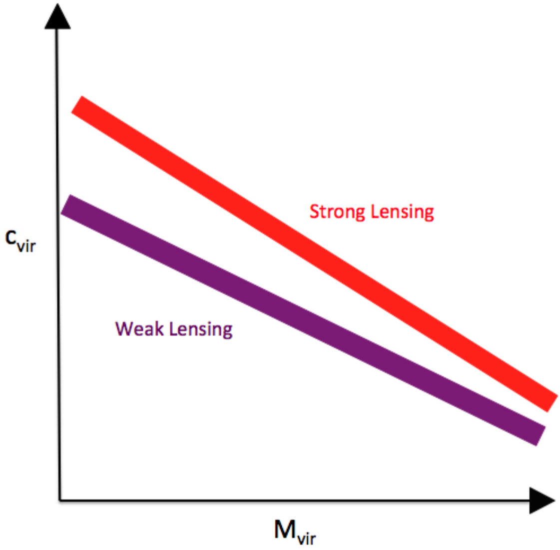

Groener, Goldberg, & Sereno (2015)

- 81 papers
- 781 cluster measurements
- 361 unique clusters
- Methods:

  (arranged roughly from small to large scale)

  - X-ray
  - Strong Lensing (SL)
  - Weak + Strong Lensing (WL+SL)
  - Weak Lensing (WL)
  - Line of sight velocity dispersion (LOSVD)
  - Caustic Method (CM)

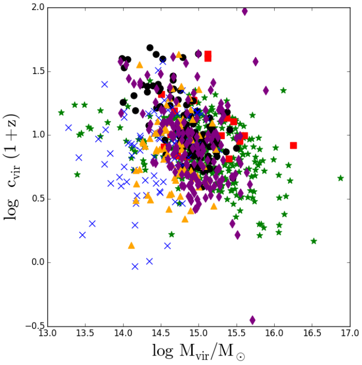

Lensing Reconstruction Techniques

Weak Lensing (WL), Strong Lensing (SL), and WL+SL

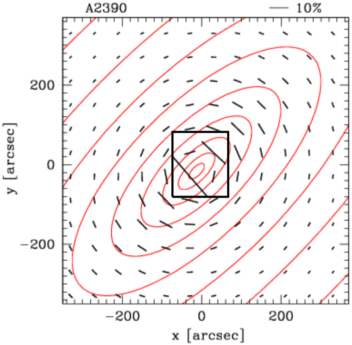

Abell 2390 (z=0.228) Oguri et al. (2010)

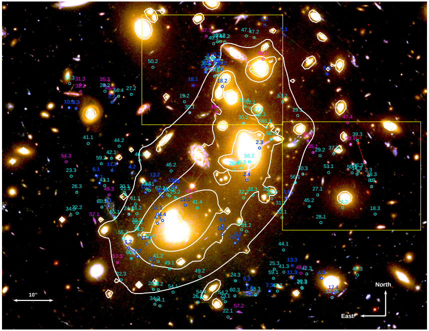

Abell 2744 (z=0.308) Jauzac et al. (2014)

Galaxy-Based Reconstruction Techniques

The Caustic Method (CM) and Line-of-sight Velocity Dispersion (LOSVD)

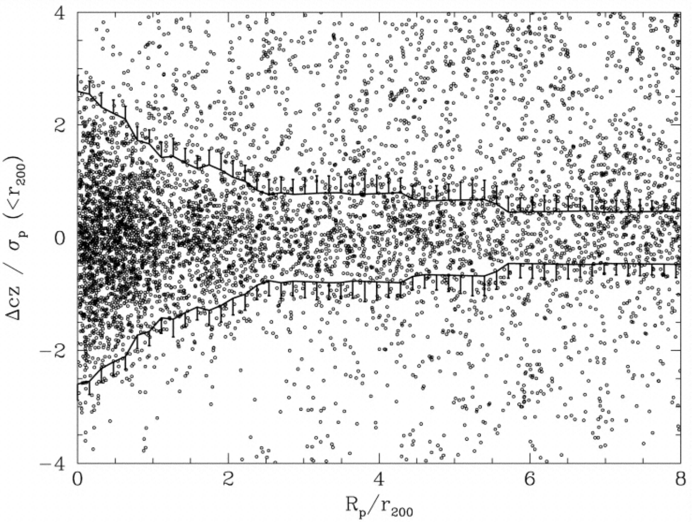

The Caustic Method Rines et al. (2006)

X-ray Reconstruction Techniques

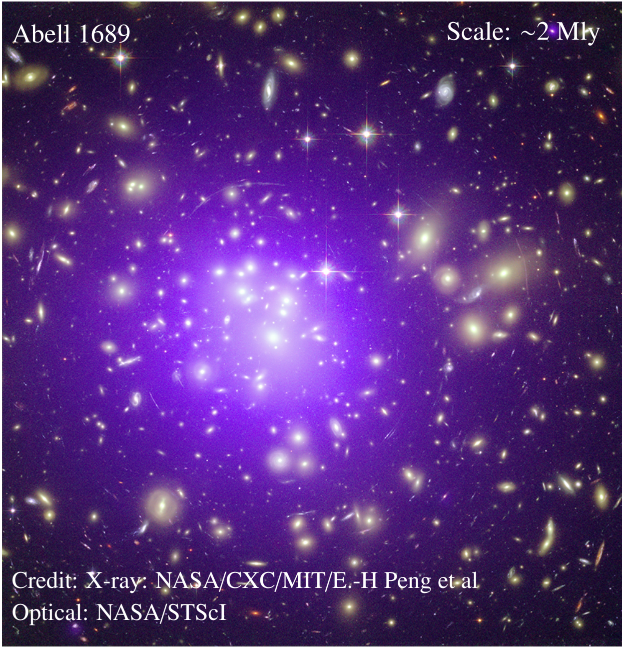

Reconstruction-Dependent Results

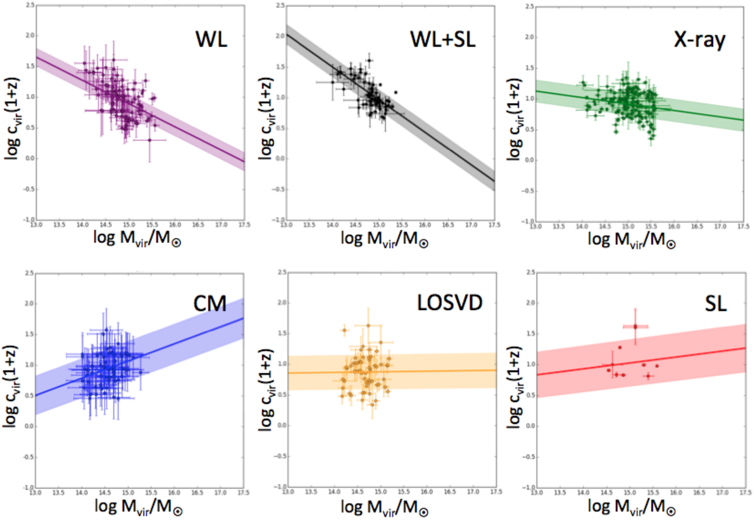

Comparison of c-M relations

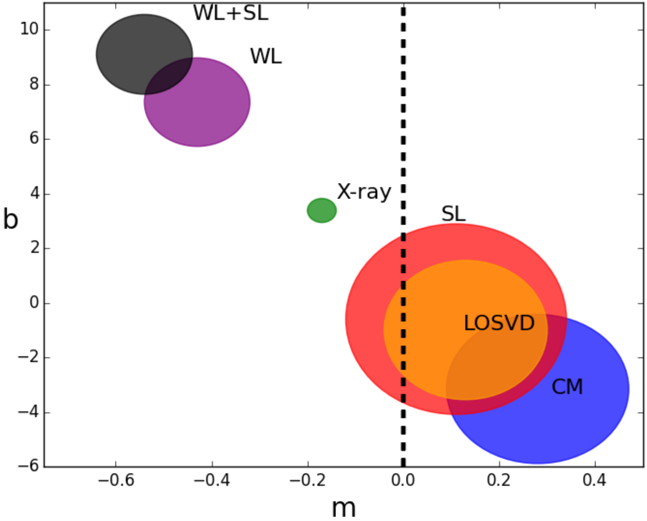

Fit To All Data

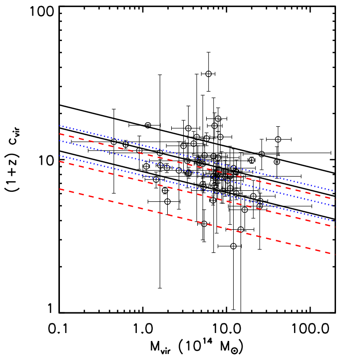

Comerford & Natarajan (2007) - All Methods.

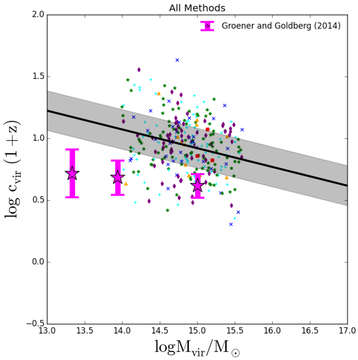

This work - All Methods.

Comparison Revisited

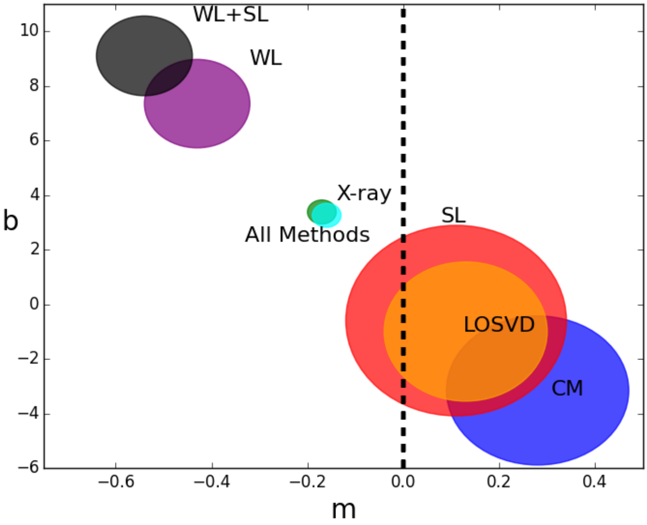

Information about the halo is lost!

Comparison With CLASH

Merten et al. (2014)

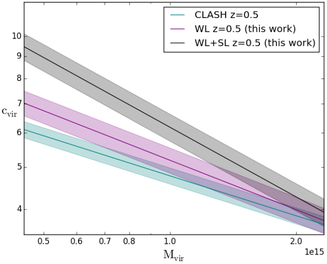

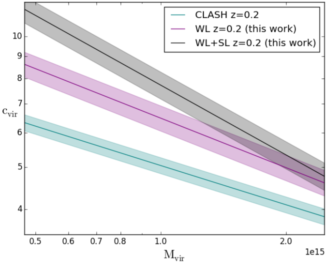

$z = 0.5$ $z = 0.2$

- Low redshift cluster concentrations are off by $\sim 50\%$ for WL, but $\sim 100\%$ for WL+SL.
- High redshift cluster concentrations are nearly in agreement with WL, but still off by $\sim 50\%$ with WL+SL.

Comparison With Simulations

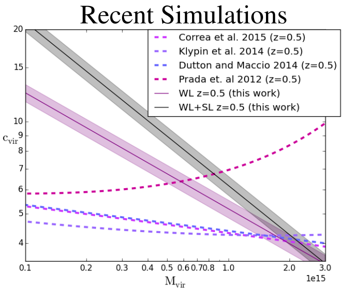

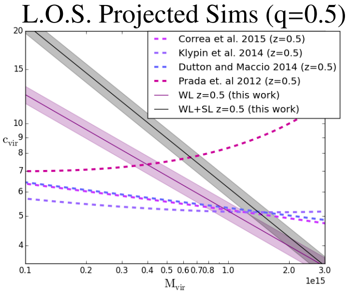

- Projection is not enough. Still off by almost a factor of 2!
- Selection effects are likely responsible.

Conclusions

- The c-M relation varies from technique to technique.
- The steepest relations are WL and WL+SL.
- The WL+SL relation is steeper (though consistent) with WL.
- The SL, CM, and LOSVD relations are not well-constrained, and are consistent with a slope of zero.

Look for us in MNRAS!

The Large-Scale Cluster Environment

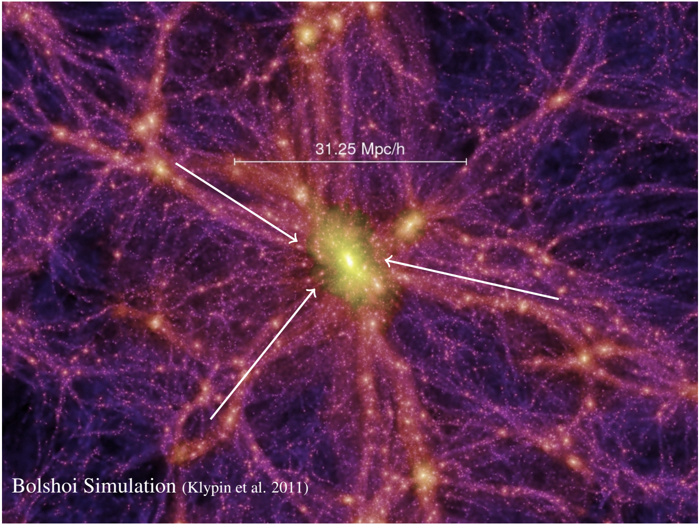

Bolshoi Simulation (Klypin et al. 2011)

The SDSS DR10 Sample

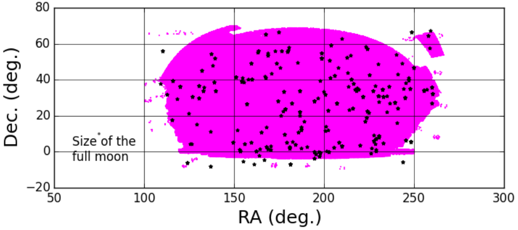

- ~ 1.4 million spectroscopically confirmed galaxies
- $z \lesssim 0.7$.
- 203 of 361 clusters are within the survey volume.

Clusters Within the LSS

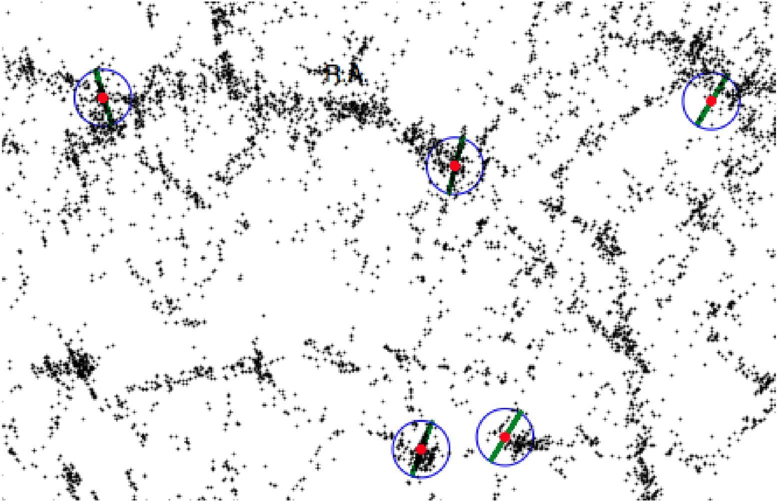

Selecting SDSS Galaxies Around Clusters

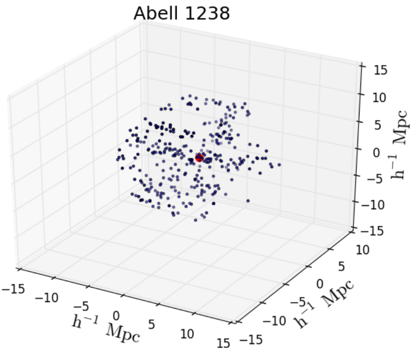

Cluster Concentration - LSS Orientation Correlation

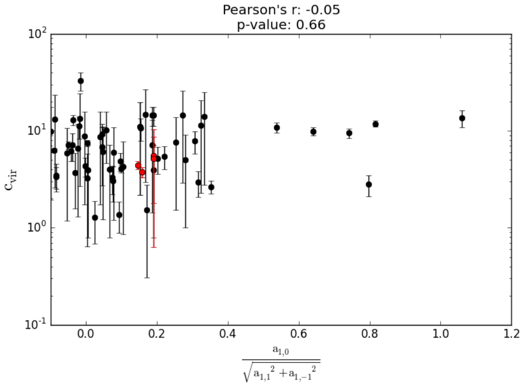

- No correlation between LSS orientation and mass and concentration.
- Techniques: WL (5), X-ray (33), CM (62), and LOSVD (34).

Future Work

- Explore alternate ways of quantifying the directionality of LSS around clusters.
- More data - particularly lensing measurements.
- Correct for redshift space distortions like Finger of God Effect, and the Kaiser Effect, which may alter the distribution of galaxies (e.g. - use cluster membership catalogs like maxBCG).

Conclusions

- Cluster halos are prolate spheroidal on small scales, and become spherical on larger scales.
- The changing of shape alters the 2D concentration on WL and SL scales differently.
- Low-mass clusters are affected by this difference the most.

- The c-M relation for clusters varies significantly from technique-to-technique.
- WL and WL+SL are the steepest relations.
- WL and WL+SL are inconsistent with theory, even after projection effects are taken into account. This likely points to selection effects as the cause.

- Cluster concentrations and masses show no correlation with the line-of-sight orientation of large scale structure (scales of $10\,h^{-1}$Mpc).

Thank you!

- Advisor: Dr. David Goldberg
- Collaborator: Dr. Mauro Sereno
- Committee: Dr. Michael Vogeley, Dr. Gordon Richards, Dr. Luis Cruz, Dr. Andrew Hicks
- Research Group (Current and Past): Justin Bird and Markus Rexroth
- My Friends and Family
- This work was also supported by the NSF (Grant 0908307).

The Connection Between c_{vir} and M_{vir}

- Low-mass halos form halos earlier than massive ones
- The core density (concentration) of the halo reflects the density of the universe at the formation time
- Since the density of the universe decreases with time, low-mass halos tend to have higher concentrations

Shape and Density profiles are obtained for all clusters which meet our selection criteria.

Density Profiles

Iterative, Moment of Inertia Tensor

$$I_{ij} = \sum w_g(\zeta) m_p (r_{i,n} - \bar{r_i})(r_{j,n} - \bar{r_j})$$

Gaussian weighting function $w_g(\zeta)$, which matches shape and orientation at each step

Model Fitting

Using Maximum-Likelihood Methods, we fit the NFW profile to halo density profiles obtained through our analysis

$$\rho_{NFW}(r) = \frac{\delta_{c_{200}} \rho_{cr}}{\frac{r}{r_s}\left(1+\frac{r}{r_s}\right)^2}$$

Cluster Timescales

- Two-Body Relaxation:

$$t_{relax} = 2 \times 10^{10} \left(\frac{V_r}{1000\, km/s} \right) \left(\frac{M_g}{10^{12} M_\odot} \right)^{-2} \left(\frac{N_d}{1000\, gal/Mpc^3} \right)^{-1}$$

  V_r is the radial component of the 3D velocity dispersion ($\approx 1000 km/s$), M_g is the mass of the galaxy (or particle), and N_d is the number of galaxies (or particles) per Mpc^3.

- Cooling Timescale:

$$\tau_{cool} = 9 \times 10^7 \, (T_8)^{1/2} \, (n_e)^{-1} \; years$$

  T_8 is the temerature in units of $10^8 K$, and n_e is measured in particles per cm^{-3} (typically $n_e \le 10^{-3}$).

- Dynamical Timescale:

$$\tau_{dyn} = 6 \times 10^{11} \left(\frac{R}{Mpc} \right) \left(\frac{V_r}{1000\, km/s} \right) years$$

Modeling The Observed c-M Relations

Power-Law Model

- $c_{vir} = \frac{A}{1+z}\left(\frac{M_{vir}}{M_*}\right)^{\alpha}$
- Constant: M_*
- Free parameters: A, α

Linear Model

- $\mathcal{Y} = m\mathcal{X} + b + \epsilon$
- $\mathcal{Y} \equiv \log c(1+z)$
- $\mathcal{X} \equiv \log M$
- $m = \alpha$
- $b = \log A - \alpha \log M_*$
- $\epsilon \sim \mathcal{N}(0, \sigma_{int})$

Measurement Uncertainty

...and other considerations.

- Arbitrary propagation of uncertainty (assuming errors are not independent):
$$\delta q \leq \left|\frac{\partial q}{\partial x}\right| + \ldots + \left|\frac{\partial q}{\partial z}\right|$$
This applies when we fit the c-M relation as a linear model (instead of the original power-law model). We also apply this for re-calculating the uncertainties for c(1 + z) (e.g. - $q = Bx$; $\delta q = |B|\delta x$).
- Best-fit values and confidence intervals to expectation values and standard deviations (D'Agostini 2004). Starting with ${\theta_m}^{\Delta_+}_{\Delta_-}$.
$$\sigma_\theta \approx \frac{\Delta_+ + \Delta_-}{2}$$
$$E[\theta] \approx \theta_m + \mathcal{O}(\Delta_+ - \Delta_-)$$

Measurement Uncertainty

...and other considerations.

- Concentation Convention: Renormalize the concentration (and mass) based upon a different definition of r_{vir} (see procedure along with fitting formulae from Hu & Kravtsov 2002).
- Correct for cosmology: We develop our own cosmology correction. This turns out to be a rather small correction (of order a few percent), unless cosmology is extremely different from the assumed fiducial cosmology $\Omega_m = 0.3$, $\Omega_\Lambda = 0.7$.

Quantifying The Angular Distribution

Spherical Harmonics

- Series: $f(\theta, \phi) = \sum_{l=0}^{\infty} \sum_{m=0}^{l} A_l^m Y_l^m(\theta, \phi)$
- $A_l^m = \frac{4\pi}{N} \sum_{i=1}^{N_{gal}} \tilde{Y_l^m}(\theta_i, \phi_i)$

$$Y_1^1 = -\sqrt{\frac{3}{8\pi}} \sin\theta \, e^{i\phi}$$

$$Y_1^0 = \sqrt{\frac{3}{4\pi}} \cos\theta$$

$$Y_1^{-1} = \sqrt{\frac{3}{8\pi}} \sin\theta \, e^{-i\phi}$$

- Compute for each cluster: $\frac{A_1^0}{\sqrt{A_1^{0\,2} + A_1^{0\,2}}}$
- A_1^0 tells us about line-of-sight direction.